



# Parallel multi-parameter study of PEI-functionalized gold nanoparticle synthesis for bio-medical applications: part 1—a critical assessment of methodology, properties, and stability

Tae Joon Cho · Justin M. Gorham ·  
John M. Pettibone · Jingyu Liu · Jiaojie Tan ·  
Vincent A. Hackley

Received: 7 December 2018 / Accepted: 26 July 2019

© This is a U.S. government work and not under copyright protection in the U.S.; foreign copyright protection may apply 2019

**Abstract** Cationic polyethyleneimine (PEI)-conjugated gold nanoparticles (AuNPs) that are chemically and physically stable under physiological conditions are an ideal candidate for certain bio-medical applications, in particular DNA transfection. However, the issue remains in reproducibly generating uniform stable species, which can cause the inadequate characterization of the resulting product under relevant conditions and timepoints. The principal objective of the present study was to develop an optimized and reproducible synthetic route for preparing stable PEI-conjugated AuNPs (Au-PEIs). To achieve this objective, a parallel multi-parametric approach involving a total of 96 reaction studies evaluated the importance of 6 key factors: PEI molar mass, PEI structure, molar ratio of PEI/Au, concentration of reaction mixtures, reaction temperature, and reaction time. Application of optimized conditions exhibited narrow size distributions with characteristic surface plasmon resonance absorption and positive surface charge. The optimized Au-PEI product generated by this study exhibits exceptional stability under a physiological isotonic medium (phosphate-buffered saline)

over 48 h and shelf-life in ambient condition without any significant change or sedimentation for at least 6 months. Furthermore, the optimized Au-PEI product was highly reproducible. Contributions from individual factors were elucidated using a broad and orthogonal characterization suite examining size and size distribution, optical absorbance, morphological transformation (agglomeration/aggregation), surface functionalities, and stability. Overall, this comprehensive multi-parametric investigation, supported by thorough characterization and rigorous testing, provides a robust foundation for the nanomedicine research community to better synthesize nanomaterials for biomedical use.

**Keywords** Gold nanoparticles · Polyethyleneimine · PEI · Positively charged gold nanoparticles · Colloidal stability · Stable gold nanoparticles · Nanobiomedicine

## Introduction

Positively charged gold nanoparticles (AuNPs) are promising materials for therapeutic applications, due to their cationic surfaces that promote cellular uptake (Arvizo et al. 2010; Cho et al. 2009; Ghosh et al. 2008; Taylor et al. 2010) and gene transfection (Chen et al. 2014; Ding et al. 2014; Elbakry et al. 2012; Lee et al. 2011a; Song et al. 2010; Thomas and Klibanov 2003). Polyethyleneimine (PEI) is the most widely used cationic polyelectrolyte for the preparation of positively

---

**Electronic supplementary material** The online version of this article (<https://doi.org/10.1007/s11051-019-4621-3>) contains supplementary material, which is available to authorized users.

T. J. Cho (✉) · J. M. Gorham · J. M. Pettibone · J. Liu ·  
J. Tan · V. A. Hackley  
Materials Measurement Science Division, National Institute of  
Standards and Technology, Gaithersburg, MD 20899, USA  
e-mail: taejoon.cho@nist.gov

charged AuNPs for such applications, due to its dual roles as reducing and stabilizing agents for gold ions (AuNP formation) (Kim et al. 2008; Note et al. 2006; Sun et al. 2005) and its chemical stability. Attractive properties for biological applications include hydrophilicity (water solubility), pH buffering efficacy (proton scavenging) (Boussif et al. 1995; Thomas and Klibanov 2003), and interaction with anionic polyelectrolytes and biological entities (e.g., cells, genes) (Kramer et al. 1998; Boussif et al. 1995). Due to these factors, there are many published reports of the synthesis and application of PEI-functionalized AuNPs (Au-PEIs).

Au-PEI can generally be prepared by two methods: (1) ligand modification (exchange or co-attachment) of AuNPs and PEI (Boyer et al. 2010; Elbakry et al. 2012; Elbakry et al. 2009; Khoury et al. 2015; Lee et al. 2011a; Rojas-Andrade et al. 2015; Sullivan et al. 2003) and (2) reduction of Au<sup>III</sup> ions in the presence of PEI (Cebrian et al. 2011; Chen et al. 2007; Chen et al. 2014; Hu et al. 2010; Kim et al. 2011; Kim et al. 2008; Kozytskiy et al. 2015; Kretschmer et al. 2014; Kuo et al. 2005; Lee et al. 2011b; Mohammed et al. 2013; Note et al. 2006; Song et al. 2010; Sun et al. 2004; Sun et al. 2005; Thiramanas and Laocharoensuk 2016; Wang et al. 2005). In general, the ligand modification method is used in layer-by-layer (LbL) assembly processes to prepare Au-PEI intermediates from negatively charged gold core (e.g., citrate-stabilized AuNPs) for RNA/DNA layering onto the Au-PEI vector (Boyer et al. 2010; Elbakry et al. 2012; Elbakry et al. 2009; Khoury et al. 2015; Pyshnaya et al. 2014; Sullivan et al. 2003). A range of PEI structures and molar masses have been utilized in effort, to create these Au-PEI intermediates. In particular, our group recently demonstrated that ligand-modified Au-PEI created through the ligand exchange method resulted in unexpected changes in surface functionality, specifically the transformation of amines to quaternary ammonium species (Cho et al. 2015). In other examples, branched PEIs on AuNPs have been used in DNA condensation reactions to create a gene delivery scaffold (Sullivan et al. 2003) for biomarker development (Khoury et al. 2015) and for gene delivery in cells after conjugation with DNA (Elbakry et al. 2012) or small interfering (si) RNA (Elbakry et al. 2009). Furthermore, PEI (branched, 0.6 kDa) can act as both reducing and stabilizing agents in aqueous and micro-emulsion systems, providing versatility in synthetic procedures that include reactions at higher temperature ( $\geq 100$  °C) (Note et al. 2006). Furthermore, linear PEI has been employed

to conjugate with cetyl-trimethylammonium bromide-capped gold nanorods and AuNPs (Pyshnaya et al. 2014).

The reduction method has been reported in the literature more frequently than the ligand modification method for preparing Au-PEI of variable sizes and using it as a direct gold core to build up multi-functional AuNPs. There are many reported examples of size-dependent physicochemical (Cebrian et al. 2011; Kim et al. 2008; Kozytskiy et al. 2015; Mohammed et al. 2013) and biological properties for Au-PEI, including toxicity (Lee et al. 2011b; Song et al. 2010), bio-uptake (Song et al. 2010; Thiramanas and Laocharoensuk 2016), and gene transfection (Cebrian et al. 2011; Chen et al. 2014; Hu et al. 2010) as well as LbL assembly (Chen et al. 2014; Song et al. 2010). However, the results have varied widely, with limited consistency from study to study when using Au-PEI generated using the reduction method. Sun et al. (2005) reported Au-PEI preparations from 25-kDa branched PEI (PEI25kB) to HAuCl<sub>4</sub> mixed together in different molar ratios at room temperature (r.t.), which resulted in particle size increasing with [PEI]/[Au] proportionally. Subsequent work by Kim et al. (2008) following Sun's method at 100 to 200 times lower concentration reported a *decrease* in Au-PEI size with increasing [PEI]/[Au]. Song et al. also employed PEI25kB and reduced HAuCl<sub>4</sub> at r.t. to obtain Au-PEIs with hydrodynamic size  $d_h \approx 15$  nm and polydispersity index (PdI)  $\approx 0.2$  (Song et al. 2010) due to different concentrations and molar ratios of reaction mixtures. On the other hand, in organic solvent (dimethylformamide) at 130 °C, Kretschmer et al. explored the synthesis of Au-PEI clusters using PEI25kB and showed that size-tuned polymer shells containing Au-PEI clusters (up to  $\approx 200$  nm in diameter) were dependent on the total concentration of reactants (Kretschmer et al. 2014). Molar mass ( $M_r$ ) variation yielded more complicated results. Mohammed et al. (2013) studied the effects of temperature, reaction time, presence/absence of reducing agent, pH, and CO<sub>2</sub> on the formation of Au-PEI using branched 0.6-kDa PEI and demonstrated the size distribution varied in a narrow range ( $\approx (4$  to  $20)$  nm) by controlling reaction conditions. Wang et al. (2005) reported that Au-PEIs obtained from the reaction with branched PEI ( $M_r$  undescribed) at 80 °C contain products that self-assemble into *dimer-* and *trimer-ic* aggregates. Thiramanas and Laocharoensuk (2016) obtained Au-PEI by reduction of gold with branched 10-kDa PEI at r.t. which has

about 30-nm size and exhibited instability in phosphate-buffered saline (PBS).

In addition to branched PEI, linear PEI can be employed to generate Au-PEI conjugates using the reduction method. For example, linear PEI (0.42 kDa) reaction with gold ions via a thermal process (Sun et al. 2004) resulted in a dominant tendency toward quasi one-dimensional aggregates. Kozytskiy et al. (2015) recently reported Au-PEI synthesis from the reduction of  $\text{NaAuCl}_4$  using linear 50-kDa PEI; their morphology and optical and catalytic properties varied significantly depend on synthetic conditions (i.e., reaction media and PEI concentration). Chen et al. (2014) employed 1.2-kDa linear PEI to prepare “sandwich-type nanocomplexes” with DNA for nucleus-targeted gene delivery.

As shown above, the variety of structures, stability, toxicity (Cebrian et al. 2011; Kim et al. 2011), and applications of Au-PEIs are well represented in the literature, but establishing coherent relationships between the concentration, PEI type, molar ratio, and other conditions or factors has been difficult to elucidate from previously reported results (Table 1). Despite the breadth and quality of previous work, it is still unclear how the specific properties of PEI and the methods utilized to conjugate it to AuNPs impact the final product size and stability (which presumably impact performance). Moreover, attempts in our laboratory to reproduce the findings from selected examples in the literature have generally yielded Au-PEI products that are inconsistent with reported results. The inconsistency of results and inability to reproduce previous work suggests the need for a systematic investigation of Au-PEI synthetic methods with respect to reaction conditions (either ligand modification or reduction method) and rigorous testing of the resulting properties. Furthermore, knowledge regarding the stability of Au-PEIs under relevant conditions is critically important for biological applications, yet this has not generally been reported in prior studies. Colloidal stability can dramatically impact the findings for bio-relevant research, where performance can be affected, for example, by one distinct population within a polydisperse material, agglomeration/aggregation effects, or surface modifications (MacCuspie 2011).

The current study evaluates the synthesis of Au-PEI by the reduction method utilizing a broad parameter space, examining 96 different reaction sets (hereafter referred as “run”) while varying (Table S1; in Electronic

Supplementary Material (ESM))  $M_r$ , PEI backbone structure, reactant concentrations, molar ratio between reactants, reaction temperature, reaction time, and the effect of a secondary reducing agent. We evaluated the Au-PEI products from each of the reaction scenarios for their optical properties, size distribution, colloidal stability in physiological buffer, and shelf-life. From this information, we identified the reaction conditions necessary to synthesize high-quality Au-PEI products by the reduction method. For the highest quality Au-PEI system, we present data on the reproducibility of the synthesis and the stability of the conjugate. As a result of this effort, a reproducible, physiologically stable Au-PEI conjugate was produced, and we have developed a synthetic blueprint for the preparation of a broad set of Au-PEI products. This comprehensive study should facilitate accelerated research advances in biological applications using Au-PEI platforms.

## Experimental section<sup>1</sup>

### Reagents

Branched 2-kDa PEI (PEI2kB, 50% mass fraction in water) and 25-kDa PEI (PEI25kB) were obtained from Sigma-Aldrich (St. Louis, MO). Branched 10-kDa PEI (PEI10kB) and linear 25-kDa PEI (PEI25kL) were obtained from Polysciences Inc. (Warrington, PA). Gold(III) chloride hydrate ( $\text{HAuCl}_4 \cdot 3\text{H}_2\text{O}$ , ACS reagent) and sodium borohydride ( $\text{NaBH}_4$ , reagent grade powder) were purchased from Sigma-Aldrich (St. Louis, MO). Phosphate-buffered saline 10 $\times$  (PBS10 $\times$ ) was obtained from HyClone (Logan, UT). PBS10 $\times$  concentrate was diluted in deionized (DI) water for stability tests. All chemicals were used without further purification. DI water (18.2 M $\Omega$  cm) was produced by an Aqua Solutions (Jasper, GA) type I biological grade water purification system.

### Measurement methods and instrumentation

Ultraviolet-visible (UV-Vis) spectra were collected on a PerkinElmer (Waltham, MA) Lambda 750 spectrophotometer equipped with an 8+8 cell changer and water-

<sup>1</sup> The identification of any commercial product or trade name does not imply endorsement or recommendation by the National Institute of Standards and Technology.

**Table 1** Summary of literature for Au-PEI synthesis using the reduction method

Reference	PEI ( $M_r$ )	$C_{PEI}^a$ (mmol/L)	$C_{HAuCl_4}^b$ (mmol/L)	$r^c$ (mol/mol)	$T^d$ (°C)	$t^e$	$d^{fs}$ (nm)	SPR (nm)	Stability <sup>h</sup>
Chen et al. (2014)	Linear (1.2 kDa)	Unknown	0.5		80	Till red	5.7 <sup>f</sup>	–	NR <sup>k</sup>
Song et al. (2010)	Branched (25 kDa)	0.055% (13.0)	13.2	≈ 1:1	r.t.	24 h	≈ 15 <sup>f</sup>	≈ 520	NR
Sun et al. (2005)	Branched (25 kDa)	480 715 860	160 120 96	3:1 6:1 9:1	r.t.	Till purple	≈ 13 <sup>g</sup> ≈ 17 <sup>g</sup> ≈ 21 <sup>g</sup>	519 538 544	NR
Kim et al. (2008)	Branched (25 kDa)	0.036% (8.4) 0.028% (6.6) 0.020% (4.8)	1.4 1.4 1.4	≈ 6:1 ≈ 4.8:1 ≈ 3.3:1	r.t.	16 h	70 ± 19 <sup>g</sup> 27 ± 7 <sup>g</sup> 10 ± 4 <sup>g</sup>	537–511	NR
Note et al. (2006)	Branched (0.6 kDa)	0.5% (120) 2.5% (600) 5% (1200) 0.091% (21.6) 0.17% (40)	1 1 1 1.82 16.7 0.24	120:1 600:1 1200:1 12:1 2.4:1 2:1	r.t. → 100 60	30 min <sup>i</sup> 20 min 20 min 3 min 2 min mins	18.9 <sup>f</sup> 19.3 <sup>f</sup> 20.9 <sup>f</sup> 9.1 <sup>f</sup> 1300 <sup>f</sup> ≈ 100 <sup>g</sup>	534 531 529 525 N/A ≈ 534, 702	NR
Sun et al. (2004)	Linear (0.4 kDa)			3:1 3.5:1 5:1 6.5:1 8:1 9.5:1			N/A N/A ≈ 25 <sup>g</sup> N/A Aggreg. Aggreg.	≈ 535 ≈ 535 ≈ 535 ≈ 535 ≈ 535 ≈ 538, 720	NR
Wang et al. (2005)	Branched (unknown)	0.96	0.24	4:1	80	1 h	–	≈ 535	NR
Cebrian et al. (2011)	Branched (25 kDa)	0.024	0.125	1:5	r.t.		≈ 6 <sup>f</sup>	–	NR
Kim et al. (2011)	Branched (25 kDa)	0.01% (2.4)	0.02 wt.% (0.5) 0.04 wt.% (1.0) 0.06 wt.% (1.5) 0.08 wt.% (2.0)	4.8:1 2.4:1 1.6:1 1.2:1	r.t.	24 h	≈ 48 <sup>f</sup> , 8 <sup>g</sup> ≈ 52 <sup>f</sup> , 14 <sup>g</sup> ≈ 48 <sup>f</sup> , 12 <sup>g</sup>	520–540	NR
Kozytskiy et al. (2015)	Linear (50 kDa)	0.0063% (1.5) 0.05% (12)	0.5	3:1 2.4:1	70	30 min	Aggreg. 30–40 <sup>g</sup> 3–7 <sup>g</sup>	535 to 540 515 to 520	NR
Kretschmer et al. (2014)	Branched (25 kDa)	0.004% (0.95) 0.04% (9.5) 0.08% (19) 0.2% (48) 0.4% (95)	0.004 wt.% (0.1) 0.04 wt.% (1.0) 0.08 wt.% (2.0) 0.2 wt.% (5.0) 0.4 wt.% (10)	9.5:1	130 (DMF)	20 min	≈ 33 <sup>g</sup> ≈ 40 <sup>g</sup> ≈ 60 <sup>g</sup> ≈ 120 <sup>g</sup> ≈ 230 <sup>g</sup>	≈ 561 ≈ 532 ≈ 532 ≈ 532 ≈ 540	NR

**Table 1** (continued)

Reference	PEI ( $M_r$ )	$C_{\text{PEI}}^a$ (mmol/L)	$C_{\text{HAuCl}_4}^b$ (mmol/L)	$r^c$ (mol/mol)	$T^d$ (°C)	$t^e$	$d^{f,g}$ (nm)	SPR (nm)	Stability <sup>h</sup>
Mohammed et al. (2013)	Branched (0.6 kDa)	0.005% (1.2) to 0.02% (4.8)	0.25	4.8:1~19:1	r.t. <sup>i</sup> 100	15 min 1 to 15 min 2 weeks	$\approx 5^g$ $\approx 12^g$ $\approx 18^g$	510 520 527	Rx. time pH values (+HCl) + CO <sub>2</sub>
Thiramanas and Laocharoensuk (2016)	Branched (10 kDa)	0.02% (4.8)	1.4	3.4:1	r.t.	16 h	$28.8 \pm 6.7^f$	$\approx 532$	in PBS (Aggreg.)

<sup>a</sup> Final concentration of PEI in reaction mixture; % represents mass fraction and molarity was calculated based on mass of repeating unit as 42 g/mol

<sup>b</sup> Final concentration of HAuCl<sub>4</sub> in reaction mixture

<sup>c</sup> Molar ratio of PEI to HAuCl<sub>4</sub> in reaction mixture

<sup>d</sup> Reaction temperature

<sup>e</sup> Reaction time

<sup>f</sup> Hydrodynamic size by DLS

<sup>g</sup> Core size by TEM

<sup>h</sup> Conditions of colloidal stability tests conducted

<sup>i</sup> After reaching 100 °C

<sup>j</sup> In presence of NaBH<sub>4</sub>

<sup>k</sup> Not reported

jacketed temperature control. Dynamic light scattering (DLS) was performed using a Malvern Instruments (Westborough, MA) Zetasizer Nano operated in 173° backscatter mode with a laser wavelength of 633 nm. Batch mode DLS measurements followed National Institute of Standards and Technology-Nanotechnology Characterization Laboratory (NIST-NCL) Protocol PCC-1 (Hackley and Clogston 2008) with  $z$ -average size ( $d_z$ ) reported as the mean of no less than five measurements plus or minus one standard deviation. Zeta potential measurements were obtained on the Zetasizer Nano using a palladium dip cell and applying the Smoluchowski equation for thin double layers. UV-Vis absorbance spectra were collected in disposable plastic semi-micro cuvettes (Brandtech, Inc., Essex, CT) with a 1-cm path length. All DLS, zeta potential, and UV-Vis measurements were conducted at  $20 \pm 0.1$  °C unless noted elsewhere. The pH was recorded with an Orion 2 Star (Thermo Scientific, Waltham, MA) using a Mettler Toledo model InLab semi-micro pH electrode with NIST traceable buffers.

Transmission electron microscopy (TEM) images were captured on a JEOL 2100 FEG operated with an accelerating voltage of 200 kV. For Au-PEIs, a drop (5  $\mu$ L to 8  $\mu$ L) of sample ( $\approx 40$   $\mu$ g/mL) was placed onto a carbon-coated copper grid (Ted Pella, Redding, CA) and dried. Particle size analysis of TEM images was performed using ImageJ (Rasband 1997), and for each sample, three regions were measured. Approximately 200 particles were measured for Au-PEI25kB products, and values are shown as a mean diameter plus or minus one standard deviation.

### Preparation of Au-PEIs

Aqueous solutions of H<sub>2</sub>AuCl<sub>4</sub> at (0.25 to 25) mmol/L were combined with PEI solutions at (0.1 to 10) mass % or (0.024 to 2.40) mol/L. Branched 2-kDa, 10-kDa, and 25-kDa PEI (PEI2kB, 10kB, and 25kB, respectively) or linear 25-kDa PEI (PEI25kL) was used to prepare Au-PEIs using various combinations of the experimental variables as specified below. Briefly, an aliquot of stock PEI solution was added to H<sub>2</sub>AuCl<sub>4</sub> solution (volume ratio,  $V_{\text{PEI}}/V_{\text{Au}} = 1/10$ ) in a borosilicate glass vial covered with a cap (EPA vials, Thermo Scientific, Waltham, MA) at r.t. (21–22 °C) with vigorous magnetic stirring ( $\approx 75$  rad/s). To examine the effect of reaction temperature, some reaction mixtures (solution in vial) were heated from r.t. to 60 °C or 80 °C using a hot plate. In

these experiments, the temperature was increased from r.t. at a rate of about 5 °C/min. For the reaction at 90 °C, aqueous H<sub>2</sub>AuCl<sub>4</sub> was heated to 90 °C; then, PEI solution was added dropwise. After desired reaction other than at r.t., hot plate was removed, and reaction mixture was cooled down to r.t. Detailed reaction conditions and results for individual experiments are listed in Table S1 of the ESM. It is important to note that (1) in heating conditions, vials were covered with caps but not tightened during reaction and (2) materials that were produced during the optimization and reproducibility studies were used for measurements of DLS and UV-Vis without purification.

### Reproducibility study

Prepare the aqueous stock solutions of H<sub>2</sub>AuCl<sub>4</sub> (2.5 mmol/L, 50 mL) and PEI25kB (10 mass %, 5 mL). Take an aliquot of 10 mL of H<sub>2</sub>AuCl<sub>4</sub> and place to a vial and stirred at room temperature. Aliquot of 1 mL from PEI stock was added to the vial and heated up to 80 °C with stirring. After reaching the desired temperature, the reaction mixture was stirred for 1.5 h. Five replicates were conducted with identical procedure. This procedure was based on “run” 3–10 except reaction time which was 30 min.

### Assignment of quality for a given “run” study generating Au-PEI materials

A value assigned to represent the quality of Au-PEI generated by the various runs employed during this study. Each quality level was assigned a name and a value (1 through 5) for the Au-PEI conjugates based on three criteria: (a) size distribution, (b) colloidal stability/shelf-life as-synthesized, and (c) physiological stability in PBS buffer. The five levels are described below:

- (1) Very poor—suspension generated from the “run” precipitated during reaction. Colloidal stability in reaction vessel (shelf-life) and in physiological media was not available.
- (2) Poor—suspension generated from the “run” was composed of stable aggregates. Au-PEI aggregates were not colloiddally stable with sedimentation occurring within a week and instantly in PBS buffer
- (3) Fair—individual Au-PEI particle formed, but in a broad size distribution. Au-PEI aggregated and

- sedimented in < 3 months under as-synthesized conditions, but still instantly sedimented in PBS buffer.
- (4) Good—Au-PEI was synthesized with a narrow size distribution ( $PdI < 0.2$ ). From a colloidal stability standpoint, a slight broadening in the size distribution was observed after 3 months with no sedimentation under as-synthesized conditions. Physiologically, Au-PEI was stable for 24+ h in PBS buffer.
  - (5) Outstanding—Au-PEI was synthesized with a narrow size distribution ( $PdI < 0.2$ ). From colloidal stability standpoint, only a slight shift was observed in the size distribution at 6 months with no sedimentation under as-synthesized conditions. Physiologically, Au-PEI was stable for 48+ h in PBS buffer.

### Uncertainty analysis

Error bars and uncertainty intervals expressed in this work, unless otherwise noted, represent one standard deviation of replicate measurements or replicate synthetic experiments, as appropriate.

## Results and discussion

### Multi-parameter controlled study and optimization

As shown in Table S1 (in ESM), we examined a large subset of experimental space for synthesizing Au-PEIs by the reduction method. In general, the framework for this multi-parameter approach was designed based on preliminary experiments in our laboratory using the original and modified methods from the literature (Table 1), ultimately leading to the design of 96 different runs for Au-PEI syntheses. Overall, to identify Au-PEIs as “outstanding quality” in this report requires (1) that they possess a narrow, stable monomodal size distribution (indicated by  $PdI < 0.2$ ) with a positive surface charge, (2) demonstrate colloidal stability (Cho et al. 2015) in physiological media for at least 48 h, and (3) maintain optical and size properties for a shelf-life up to 6 months.

In the case of branched 2-kDa PEI, most “run” studies resulted in a broad size distribution of Au-PEI, with the exception of high molar ratio of  $[PEI2kB]/[Au]$  ( $r^{PEI/Au} > 96$  at r.t. (Table S1), which resulted in no visible reduction to form Au particles. All Au-PEI2kBs were of

fair quality, exhibiting a short shelf-life ( $\leq 2$  months) and were completely unstable in PBS, as characterized by immediate precipitation and sedimentation (“run” 1–1 to 1–16, Table S1). These findings revealed no clear trends in synthesizing Au-PEI conjugates of even fair quality, suggesting an inherent instability in the Au-PEI2kB system. Synthesis involving the larger molar mass PEI10kB generally exhibited improved stability compared with PEI2kB. Some clear trends emerged with respect to optimizing experimental parameters. For example, Au-PEI10kB products obtained by gradual heating (from r.t. to 80 °C) yielded narrower size distributions than those synthesized at r.t. or 90 °C. Additionally, the colloidal stability of Au-PEI10kB improved when synthesized with increasing reaction temperature ( $90\text{ °C} \geq T \geq 60\text{ °C}$ ) (“run” 2–1 to 2–11, Table S1). Experiments using the largest molar mass PEI25kB series showed greatest colloidal and physiological stability. Consistent with literature and our preliminary studies using PEI25kB, reduction of gold chloride occurred over a range of temperatures resulting in narrower size distributions with improved stability compared with the smaller molar mass branched PEIs. In the following subsections, we evaluate more closely the contributions from each parameter (Fig. 1) and discuss the mechanisms governing the observed results.

### $M_r$ of branched PEIs

The molar mass effect for branched PEIs (Fig. 1a) can be explained by the “nesting” effect, which is illustrated in Fig. 2. Unlike the formation of Au-PEIs by ligand exchange, in the reduction method, PEI chains trap gold ions ( $Au^{III}$ ) inside the branched structure, where reduction of  $Au^{III}$  by the amine occurs resulting in the nucleation of nanoscale clusters/particles. During this process, larger PEIs produce Au-PEIs that are well dispersed due to a thick surrounding nest of PEI that provides stable space until the reduction/clustering process is complete and prevents particle-particle interactions (agglomeration) and core fusion or sintering (aggregation). If the nest is smaller, the repulsive force may be insufficient to inhibit particle-particle interactions (Fig. 2, bottom row) during reduction, which would result in the previously reported colloidal instabilities (Kretschmer et al. 2014).

Based on the current findings, use of higher  $M_r$  PEI generally resulted in higher quality Au-PEI, characterized as narrower in size distribution and greater shelf-

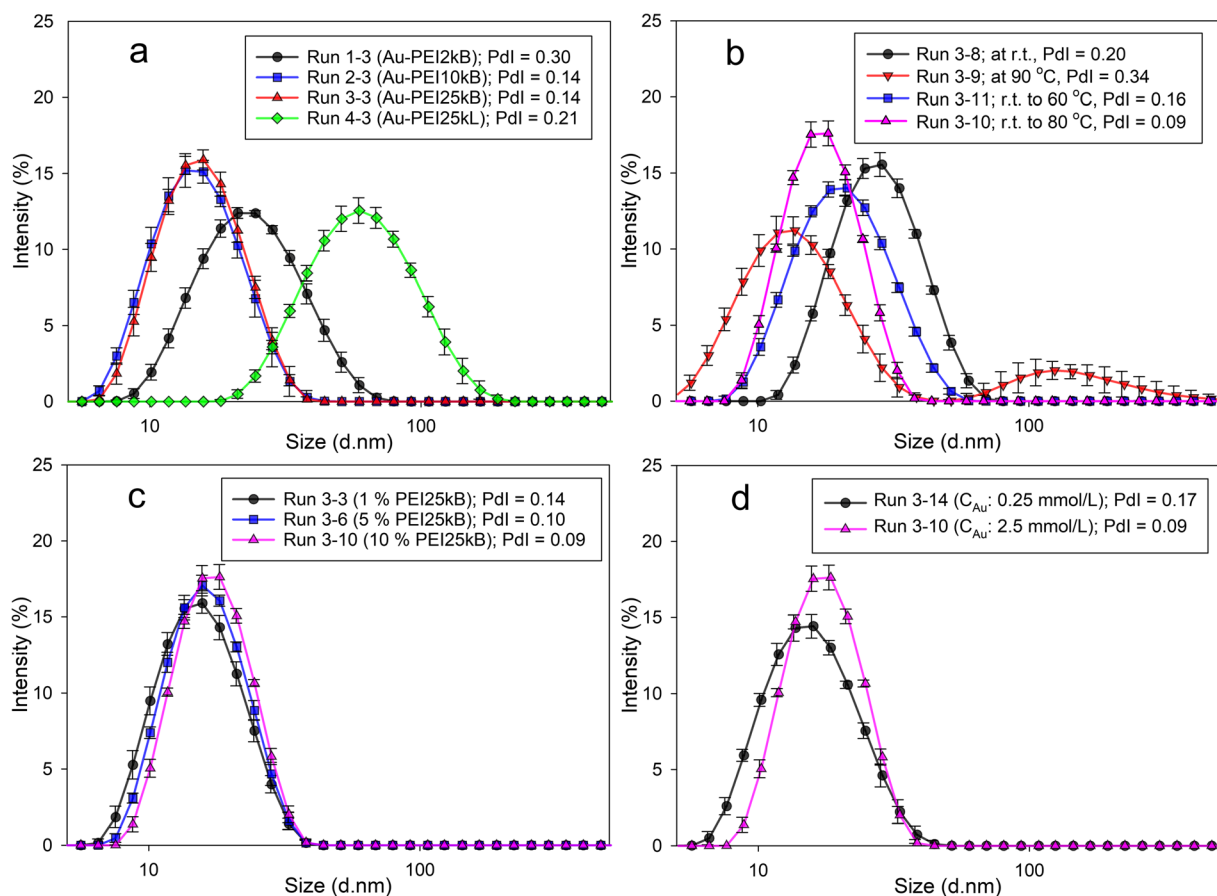


**Fig. 1** Representative DLS histograms of the impacts of different parameters on the size and size distribution upon completion of the synthetic process, including **a** molar mass and structure of PEI, **b** reaction temperature, **c** molar ratio of PEI to HAuCl<sub>4</sub> at fixed gold

concentration, and **d** gold concentration at fixed molar ratio to PEI. Error bars and uncertainty intervals expressed in this work, unless otherwise noted, represent one standard deviation of replicate measurements or replicate synthetic experiments, as appropriate

life and physiological stability. Notably, in terms of size/size distribution and shelf-life for a certain period, Au-PEI10kB and PEI25kB showed very similar results. However, colloidal stability in physiological media is quite distinguishable (see ESM Figure S1).

### Temperature

The impact of temperature on Au-PEI quality was evaluated by examining products formed using four different temperature programs: constant r.t., constant 90 °C, ramping from r.t. to 60 °C, and ramping from r.t. to 80 °C (Fig. 1b). For the “ramping” experiments, temperature was increased from r.t. at a rate of about 5 °C/min. At r.t., reaction times required for Au-PEI formation were consistently > 12 h, based on the observation of a color change in the solution (see Table S1).

Here, the protracted reaction time is attributed to the higher activation energy barrier for Au<sup>III</sup> to Au<sup>0</sup> reduction in the absence of a stronger reducing agent (e.g., sodium borohydride) (Mohammed et al. 2013). In contrast, at 90 °C, the reduction rate was dramatically enhanced, but the resulting Au-PEI size distribution was broad, as characterized by an increased Pdl and purple color. The poor quality is likely due to PEI having insufficient time to complete the stable protonation/complexation steps at the beginning of the reduction. Using ramping temperature programs to a final temperature of 60 or 80 °C, most of the prepared Au-PEI systems (except some PEI2kB products) yielded narrower size distributions (lower Pdl) than those at constant temperatures (at r.t. and 90 °C). While there were some variations depending on other experimental variables (described below), generally speaking

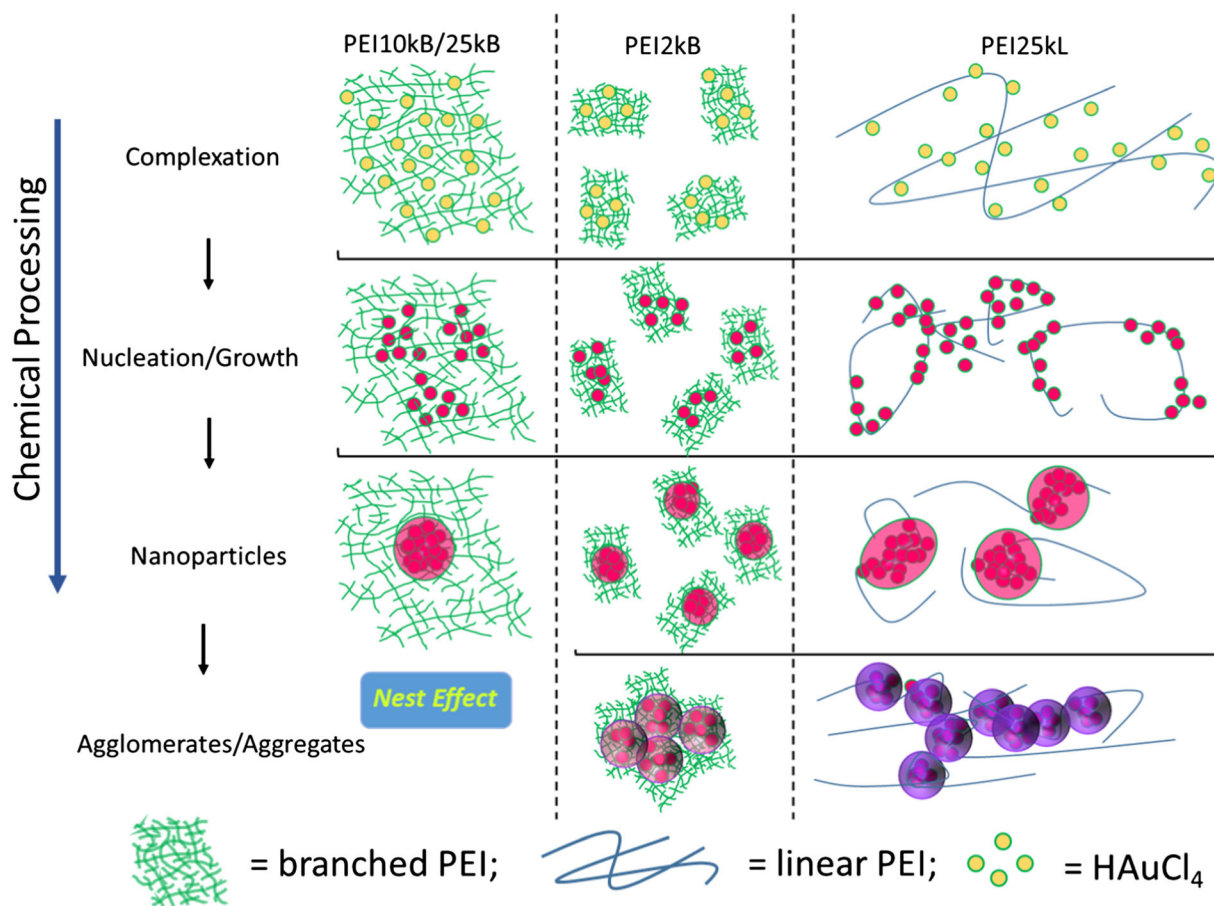


**Fig. 2** Illustration of the relationship between ligand and morphology of Au-PEIs (nest effect) induced by  $M_r$  and backbone structure of PEIs during Au-PEI formation

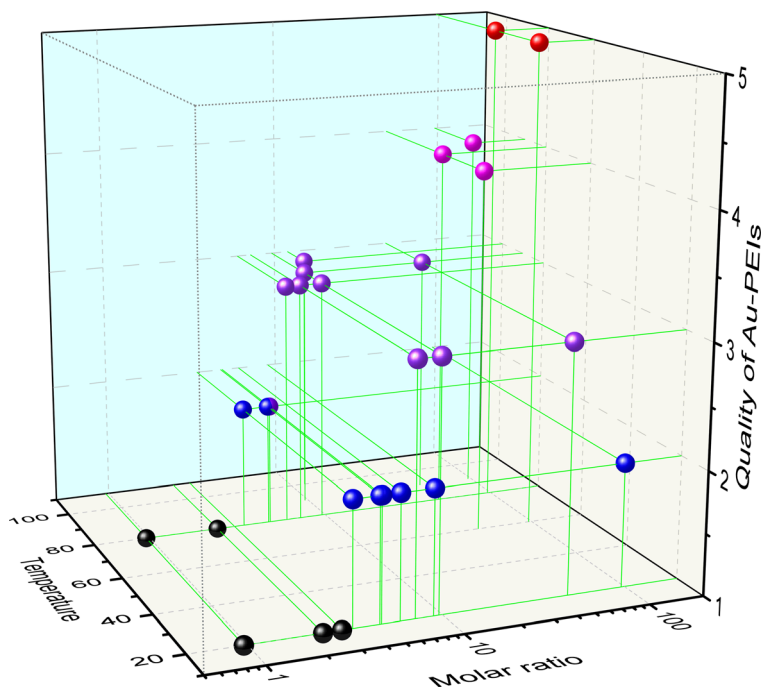
the narrowest distributions and the highest quality Au-PEI particles were formed by ramping the temperature from r.t. to 80 °C. Results of ramping from r.t. to 60 °C exhibited similar PDI values indicating narrow size distribution with those from r.t. to 80 °C, but yielded lower optical density (SPR band; data omitted).

Molar ratio of reactants,  $r^{\text{PEI/Au}}$

General observations with respect to concentration and molar ratio were that reactions with higher  $r^{\text{PEI/Au}}$  (from 9.6 to 96,  $C^{\text{Au}} = 2.5$  mmol/L) required longer reaction times and either formed unstable species or no detectable Au-PEI formation for synthesis conditions at low  $M_r$  and extreme temperature conditions (e.g., r.t. and 90 °C). The higher the  $M_r$  of the employed PEI in the synthesis approach, the less dependent the reaction was on  $r^{\text{PEI/Au}}$  regardless of temperature (Fig. 1c). However, the quality of Au-

PEI products for runs based on ramping temperature from r.t. to 80 °C was strongly dependent upon the molar ratios, especially for 25-kDa PEI (see Fig. 3). The optimized combination of  $C^{\text{Au}}$  and  $r^{\text{PEI/Au}}$  in this study was found to be 2.5 mmol/L and 96, respectively, which resulted in the highest quality products (2–10, 3–10, in ESM Table S1) for PEI10kB and PEI25kB. A potential reason for the low quality of Au-PEI at low  $r^{\text{PEI/Au}}$  is that low concentration of PEI may not provide sufficient reducing activity to complete clustering/stabilizing for Au-PEI25kB formation. Indeed, even the lower range of  $r^{\text{PEI/Au}}$  products for optimized temperature programs of r.t. to 80 °C (“run” 3–21 to 24, in ESM Table S1) and r.t. (“run” 3–17 to 20, in ESM Table S1), these yielded similar results in terms of both poor quality and stability. Notably, runs (3–44 to 46) demonstrate that too much PEI (e.g.,  $r^{\text{PEI/Au}} > 100$ ) is also problematic and resulted in broad size distributions of Au-PEI25kBs.

**Fig. 3** Relationship between molar ratio ( $r^{\text{PEI/Au}}$ ), temperature, and product quality for Au-PEI25kB, where  $0.96 \leq r^{\text{PEI/Au}} \leq 96$  and  $C^{\text{Au}} \approx (1.4 \text{ to } 2.5) \text{ mmol/L}$  were examined. Description of quality scale (1 to 5) is given in the “Experimental section”



Based on the comparison of different synthesis conditions controlling for  $M_r$ , temperature, and  $r^{\text{PEI/Au}}$ , we conclude that the reaction conditions are optimized using  $M_r$  PEI at a relatively high  $r^{\text{PEI/Au}}$  and Au concentrations below 10 mmol/L with temperature ramping from r.t. to 80 °C. The relationship between  $r^{\text{PEI/Au}}$ , temperature, and product quality is illustrated in Fig. 3 (for Au-PEI25kB and for  $C^{\text{Au}} \approx$

1.4 to 2.5 mmol/L). Figure 4 shows the  $z$ -average hydrodynamic size/size distribution ( $d_z = 16.2 \pm 0.14 \text{ nm}$  (gold core + PEI coating thickness) by DLS, left panel a) with positive zeta-potential ( $z-p$ ) value (by DLS;  $z-p = + (22.7 \pm 2.2) \text{ mV}$  at pH 9 ( $10\times$  dilution in DI water)), the optical absorbance spectrum (by UV-Vis, middle panel b), and gold core size (( $8.6 \pm 2.3) \text{ nm}$ )/shape uniformity (by TEM, right

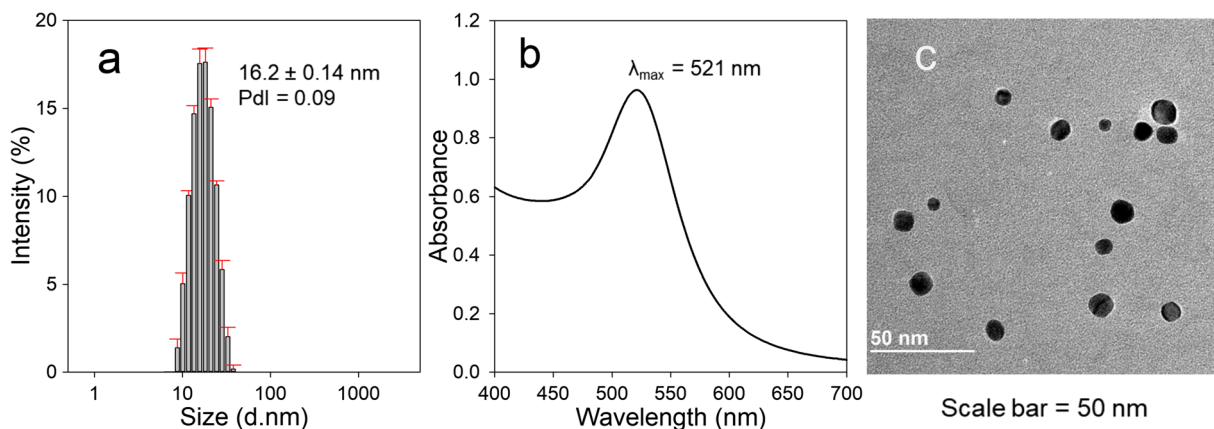


**Fig. 4** Data of representative Au-PEI25kB prepared by reaction “run” 3–10; in a temperature regime ramping from r.t. to 80 °C,  $r^{\text{PEI/Au}} = 96$ ,  $C^{\text{Au}} = 2.5 \text{ mmol/L}$ ; **a**  $z$ -average hydrodynamic size and size distribution by DLS, **b** SPR band by UV-Vis, and **c** shapes and core sizes (( $8.6 \pm 2.3) \text{ nm}$ ) by TEM. For DLS and UV-Vis, samples were diluted in DI water (dilution factor = 10) before

measurements. The unit of size (d. nm) represents diameter. Error bars on size histogram by DLS (**a**) represent one standard deviation ( $\pm 0.14$  in here) of 5 replicate measurements of one Au-PEI25kB sample. For the size analysis by TEM, 188 particles of Au-PEI25kB were measured and values are shown as a mean diameter plus or minus one standard deviation

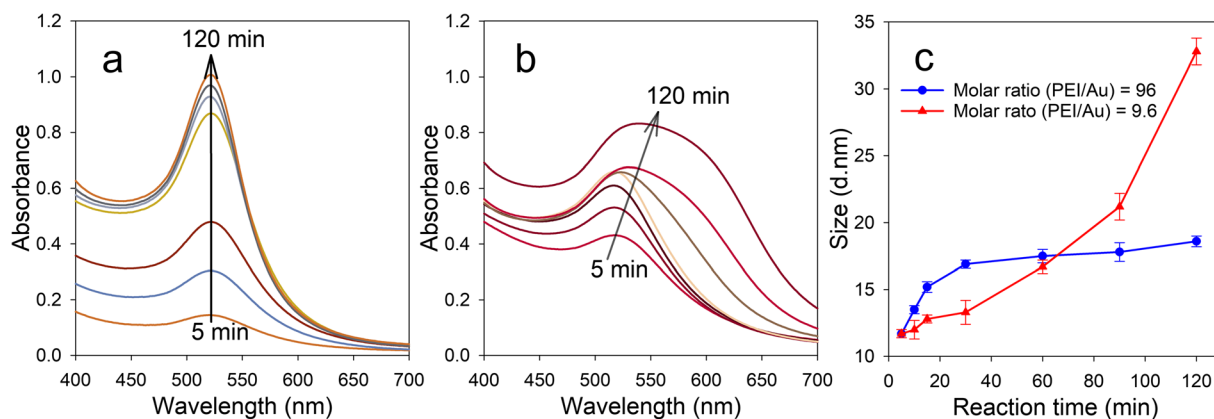


**Fig. 5** Effect of reaction time on Au-PEI25kB synthesis after ramping to 80 °C and dependence on molar ratio ( $r^{\text{PEI/Au}}$ ) at  $C^{\text{Au}}$  is 2.5 mmol/L. Change of absorbance spectra (guided by arrows)

of reaction mixtures with a  $r^{\text{PEI/Au}} = 96$ , **b**  $r^{\text{PEI/Au}} = 9.6$  by UV-Vis monitoring, and **c** change of  $d_z$  (square:  $r^{\text{PEI/Au}} = 96$ , triangle:  $r^{\text{PEI/Au}} = 9.6$ , monitored by DLS) in accordance with reaction time

panel c) for Au-PEI25kB in “run” (3–10), as the most promising reaction condition. DLS can be defined a “wet” method for size determination and it provides hydrodynamic size of the tested nanoparticles. On the other hand, TEM is a “dry” method to visualize and measure the hard core size and shape of said particles. Hence, TEM yields the gold core size of Au-PEI, while DLS yields the effective hydrodynamic size, including any water or ligands that are associated with the surface. The latter is generally larger than the former, on average. This is, in fact, what we find in this study. The product also exhibited colloidal stability (Cho and Hackley 2018) in as-synthesized and physiological media (up to 6 months of shelf-life in DI water and least 48 h in PBS, respectively, Figure S2 in ESM).

#### Effect of reaction time regarding molar ratio

Using “run” (3–10) selected from previously discussed results and based on optimization of multiple factors (PEI25kB,  $C^{\text{Au}} = 2.5$  mmol/L and reaction temperature ramping from r.t. to 80 °C), the effect of reaction time was then evaluated over a range of  $r^{\text{PEI/Au}}$  from 9.6 to 96. For a precise evaluation in this study, reaction time was counted right after the reaction temperature reached 80 °C. To monitor changes over time, PdI and  $d_z$  were measured and colloidal stability was assessed by monitoring the SPR band (Fig. 5, Table S2 in ESM). At relatively high  $r^{\text{PEI/Au}}$  (96 and 48), results indicate that hydrodynamic size initially increases steeply then slows substantially at long reaction times (>20 min). Coincidentally, the PdI decreases and the SPR band at  $\lambda_{\text{max}}$

increases in magnitude at a constant wavelength with reaction time (see Fig. 5a), expressing similar fast and slow growth regimes.

At relatively low  $r^{\text{PEI/Au}}$  (9.6), the reaction time dependence is markedly different, with the hydrodynamic size increasing more rapidly at the reaction’s end stage (see Fig. 5b,  $t > 80$  min). Additionally, the absorbance spectra show a concomitant red shift and substantial broadening/distortion with increasing time. This suggests that different growth mechanisms or limiting effects are in play at high versus low PEI to Au ratios. At low ratios, the quality and stability deteriorate rapidly after roughly 30 min; this is evidenced by a change in color of the suspension from red to purple after 120 min and the distortion of the SPR peak. Initially (up to about 30 min), the size and SPR bands are similar. Taken together, these results suggest that initially formed nucleation products are probably similar, but subsequent growth likely occurs through a surface catalyzed reaction that requires increased PEI concentrations for product stabilization (Finney and Finke 2008; Polte et al. 2010). This result confirms the importance of controlling  $r^{\text{PEI/Au}}$ , as we evaluated in the “Results and discussion” section, and highlights it as a dominant factor in the Au-PEI synthesis.

#### Additional observations: poor average size control, and poor qualities with linear PEI, and branched PEI/NaBH<sub>4</sub>

After evaluating the 96 runs, it was determined that the size of the Au-PEIs was significantly impacted by

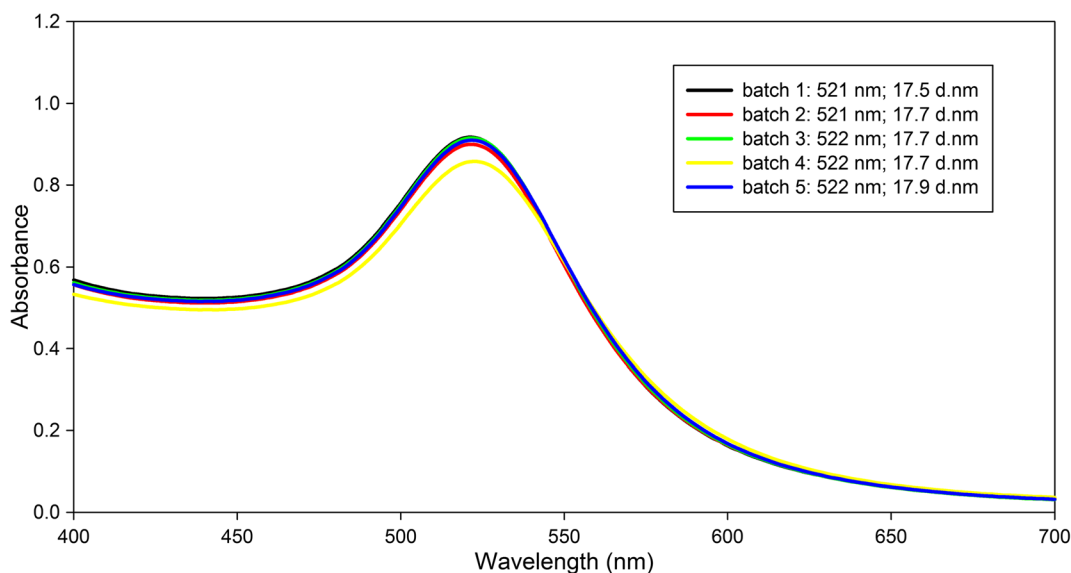


**Fig. 6** Reproducibility of Au-PEI25kB prepared using the optimized “run” in 10-mL scale reactions; UV-Vis absorbance spectra are shown. The inset lists the values of  $\lambda_{\max}$  and the mean z-average (hydrodynamic) diameter for each replicate reaction

changes in parameters, yet there were no clear systematic trends, which confirms previous reports about the sensitive nature of the synthesis (Finney and Finke 2008; Polte et al. 2010). Briefly, we found that conditions involving lower  $r^{\text{PEI/Au}}$  ( $\approx 3 \leq r^{\text{PEI/Au}} \leq \approx 9$ ) formed larger sizes and size distributions for a range  $C^{\text{Au}}$  ( $\approx 1 \leq C^{\text{Au}} \leq \approx 2.5$  mmol/L) at room temperature (“run” 3–17, 18, 27–30, 41, 42, Table S1; Figure S2, in ESM); however, this was only observed for a narrow range of  $r^{\text{PEI/Au}}$  or  $C^{\text{Au}}$  values and mostly led to inconclusive size distributions/average size or even precipitates.

With respect to linear PEI, we evaluated the effect of PEI backbone structure by comparing results for linear PEI (25 kDa, PEI25kL) with the branched PEI discussed in detail above. Interestingly, the identical condition for Au-PEI25kB (3–10, Table S1) generated precipitates of Au-PEI25kL (4–5, Table S1) during the reaction. Generally, linear PEI has not been successfully used to prepare Au-PEI conjugates for bio-medical applications, and the results obtained in the present study, and summarized in Table S1 (“run” 4–1 to 7), attest to this fact.

Lastly, the effect of additional reducing agent ( $\text{NaBH}_4$ ) was evaluated (reaction runs 5–1–9). All reactions with PEI2kB resulted in precipitation within 10-min stirring (5–1–3, Table S1). The attempts with PEI10kB (5–4–6, Table S1) and PEI25kB (5–7–9, Table S1) exhibited a brown color with multi-modal size distributions by DLS and very broad SPR bands in

common by UV-Vis (data omitted) after stirring over 20 h.

### Reproducibility

Determining the optimal conditions for a synthetic reaction, as demonstrated in Fig. 3, is only meaningful if the reaction is robust and reproducibility can be clearly demonstrated. Using synthesis conditions described in the “Experimental section” and based on “run” 3–10 in the ESM (but 1.5-h reaction time), reproducibility was evaluated to determine the practical viability of this synthetic process via conducting 10-mL batch reactions and replicating five times. As illustrated in Fig. 6, this synthetic procedure yielded excellent reproducibility in Au-PEI product generated, with an average hydrodynamic size of  $17.7 \pm 0.1$  nm and optical absorbance spectra with SPR maximum ( $\lambda_{\max}$ ) at  $521.6 \pm 0.55$  nm. The peak maximum absorbance had a coefficient of variation of 2.7%.

### Conclusions

A thorough investigation of Au-PEIs synthesized by the reduction method has been conducted using a multi-parameter approach controlling variables, including PEI  $M_n$ , PEI backbone structure,  $r^{\text{PEI/Au}}$ , concentrations

of Au and PEI, temperature, and reaction time. This study demonstrates that employing 25-kDa branched PEI and 2.5 mmol/L of  $C^{Au}$  at a  $r^{PEI/Au} = 96$  and a temperature ramping program of r.t. to 80 °C for  $\approx$  (1.5 to 2) h (after reaching the desired temperature) is the most optimal conditions for the preparation of high-quality Au-PEIs. Under these conditions, Au-PEI conjugates were characterized by a narrowness in size distribution (nominal 20 nm of hydrodynamic size), long-term colloidal stability in as-synthesized conditions, and colloidal stability in physiologically relevant conditions. Aside from stability and a narrow size distribution, this set of reaction condition revealed shape uniformity and positive surface charge (surface functionality). Additionally, this optimized template for Au-PEI synthesis was highly reproducible in terms of hydrodynamic diameter and optical properties. Recommended general guidelines for tailoring a synthetic approach for high-quality Au-PEI are as follows:

- Branched PEI (25 kDa) is preferable to linear PEI
- $M_r$  selection: 25 kDa > 10 kDa > 2 kDa
- $r^{PEI/Au} \approx 96$
- Temperature ramping from r.t. to 80 °C
- $\approx$  1.5~2 h of reaction time after reaching the desired temperature

Ultimately, the Au-PEI25kB produced in this study could be a successful candidate for biological application due to its cationic properties. However, complete characterization of physicochemical properties of these optimized nanomaterials is critical to correlate and predict with biological behaviors. The determination of Au-PEI's physicochemical properties and their relationships with colloidal stability are the subject of ongoing studies and will be reported in the follow-up to this manuscript.

#### Compliance with ethical standards

**Conflict of interest** The authors declare that they have no conflict of interest.

#### References

- Arvizo RR, Miranda OR, Thompson MA, Pabelick CM, Bhattacharya R, Robertson JD, Rotello VM, Prakash YS, Mukherjee P (2010) Effect of nanoparticle surface charge at the plasma membrane and beyond. *Nano Lett* 10(7):2543–2548. <https://doi.org/10.1021/nl101140t>
- Boussif O, Lezoualch F, Zanta MA et al (1995) A versatile vector for gene and oligonucleotide transfer into cells in culture and in-vivo - polyethylenimine. *Proc Natl Acad Sci U S A* 92(16):7297–7301
- Boyer C, Bousquet A, Rondolo J, Whittaker MR, Stenzel MH, Davis TP (2010) Glycopolymer decoration of gold nanoparticles using a LbL approach. *Macromolecules* 43(8):3775–3784
- Cebrian V, Martin-Saavedra F, Yague C, Arruebo M, Santamaria J, Vilaboa N (2011) Size-dependent transfection efficiency of PEI-coated gold nanoparticles. *Acta Biomater* 7(10):3645–3655
- Chen CC, Hsu CH, Kuo PL (2007) Effects of alkylated polyethylenimines on the formation of gold nanoplates. *Langmuir* 23(12):6801–6806
- Chen ZZ, Zhang LF, He YL, Li YF (2014) Sandwich-type Au-PEI/DNA/PEI-Dexa nanocomplex for nucleus-targeted gene delivery in vitro and in vivo. *ACS Appl Mater Interfaces* 6(16):14196–14206. <https://doi.org/10.1021/am503483w>
- Cho TJ, Hackley VA (2018) Assessing the chemical and colloidal stability of functionalized gold nanoparticles NIST special publication 1200–26. National Institute of Standards and Technology <https://nvlpubs.nist.gov/nistpubs/SpecialPublications/NIST.SP.1200-26.pdf>. Accessed June 2018
- Cho EC, Xie JW, Wurm PA, Xia YN (2009) Understanding the role of surface charges in cellular adsorption versus internalization by selectively removing gold nanoparticles on the cell surface with a I-2/KI etchant. *Nano Lett* 9(3):1080–1084
- Cho TJ, Pettibone JM, Gorham JM, Nguyen TM, MacCuspie RI, Gigault J, Hackley VA (2015) Unexpected changes in functionality and surface coverage for au nanoparticle PEI conjugates: implications for stability and efficacy in biological systems. *Langmuir* 31(27):7673–7683. <https://doi.org/10.1021/acs.langmuir.5b01634>
- Ding Y, Jiang ZW, Saha K, Kim CS, Kim ST, Landis RF, Rotello VM (2014) Gold nanoparticles for nucleic acid delivery. *Mol Ther* 22(6):1075–1083. <https://doi.org/10.1038/mt.2014.30>
- Elbakry A, Zaky A, Liebl R, Rachel R, Goepferich A, Breunig M (2009) Layer-by-layer assembled gold nanoparticles for siRNA delivery. *Nano Lett* 9(5):2059–2064
- Elbakry A, Wurster EC, Zaky A, Liebl R, Schindler E, Bauer-Kreisel P, Blunk T, Rachel R, Goepferich A, Breunig M (2012) Layer-by-layer coated gold nanoparticles: size-dependent delivery of DNA into cells. *Small* 8(24):3847–3856. <https://doi.org/10.1002/smll.201201112>
- Finney EE, Finke RG (2008) Nanocluster nucleation and growth kinetic and mechanistic studies: a review emphasizing transition-metal nanoclusters. *J Colloid Interface Sci* 317(2):351–374. <https://doi.org/10.1016/j.jcis.2007.05.092>
- Ghosh P, Han G, De M, Kim CK, Rotello VM (2008) Gold nanoparticles in delivery applications I. *Adv Drug Deliv Rev* 60(11):1307–1315
- Hackley VA, Clogston JD (2008) Measuring the size of nanoparticles in aqueous media using batch-mode dynamic light scattering. In: National Cancer Institute, Nanotechnology characterization laboratory [http://ncl.cancer.gov/working\\_assay-cascade.asp](http://ncl.cancer.gov/working_assay-cascade.asp). [http://ncl.cancer.gov/working\\_assay-cascade.asp](http://ncl.cancer.gov/working_assay-cascade.asp). Accessed Nov 2007

- Hu C, Peng Q, Chen FJ, Zhong ZL, Zhuo RX (2010) Low molecular weight polyethylenimine conjugated gold nanoparticles as efficient gene vectors. *Bioconjug Chem* 21(5): 836–843
- Khoury LR, Goldbart R, Traitel T, Enden G, Kost J (2015) Harvesting low molecular weight biomarkers using gold nanoparticles. *ACS Nano* 9(6):5750–5759. <https://doi.org/10.1021/nn507467y>
- Kim K, Lee HB, Lee JW, Park HK, Shin KS (2008) Self-assembly of poly(ethyleneimine)-capped au nanoparticles at a toluene-water interface for efficient surface-enhanced Raman scattering. *Langmuir* 24(14):7178–7183
- Kim EJ, Yeum JH, Ghim HD, Lee SG, Lee GH, Lee HJ, Han SI, Choi JH (2011) Ultrasmall polyethyleneimine-gold nanoparticles with high stability. *Polymer-Korea* 35(2):161–165
- Kozytskiy AV, Raevskaya AE, Stroyuk OL, Kotenko IE, Skorik NA, Kuchmiy SY (2015) Morphology, optical and catalytic properties of polyethyleneimine-stabilized au nanoparticles. *J Mol Catal A-Chem* 398:35–41. <https://doi.org/10.1016/j.molcata.2014.11.017>
- Kramer G, Buchhammer HM, Lunkwitz K (1998) Investigation of the stability of surface modification by polyelectrolyte complexes - influence of polyelectrolyte complex components and of substrates and media. *Colloids Surf A-Physicochem Eng Asp* 137(1–3):45–56. [https://doi.org/10.1016/s0927-7757\(97\)00385-3](https://doi.org/10.1016/s0927-7757(97)00385-3)
- Kretschmer F, Mansfeld U, Hoepfner S, Hager MD, Schubert US (2014) Tunable synthesis of poly(ethylene imine)-gold nanoparticle clusters. *Chem Commun* 50(1):88–90. <https://doi.org/10.1039/c3cc45090b>
- Kuo PL, Chen CC, Jao MW (2005) Effects of polymer micelles of alkylated polyethylenimines on generation of gold nanoparticles. *J Phys Chem B* 109(19):9445–9450
- Lee MY, Park SJ, Park K, Kim KS, Lee H, Hahn SK (2011a) Target-specific gene silencing of layer-by-layer assembled gold-cysteamine/siRNA/PEI/HA nanocomplex. *ACS Nano* 5(8):6138–6147
- Lee Y, Lee SH, Kim JS, Maruyama A, Chen XS, Park TG (2011b) Controlled synthesis of PEI-coated gold nanoparticles using reductive catechol chemistry for siRNA delivery. *J Control Release* 155(1):3–10
- MacCuspie RI (2011) Colloidal stability of silver nanoparticles in biologically relevant conditions. *J Nanopart Res* 13(7):2893–2908. <https://doi.org/10.1007/s11051-010-0178-x>
- Mohammed FS, Cole SR, Kitchens CL (2013) Synthesis and enhanced colloidal stability of cationic gold nanoparticles using polyethyleneimine and carbon dioxide. *ACS Sustain Chem Eng* 1(7):826–832. <https://doi.org/10.1021/sc400028t>
- Note C, Kosmella S, Koetz J (2006) Poly(ethyleneimine) as reducing and stabilizing agent for the formation of gold nanoparticles in w/o microemulsions. *Colloids Surf A-Physicochem Eng Asp* 290(1–3):150–156
- Polte J, Herder M, Erler R, Rolf S, Fischer A, Würth C, Thünemann AF, Kraehnert R, Emmerling F (2010) Mechanistic insights into seeded growth processes of gold nanoparticles. *Nanoscale* 2(11):2463–2469. <https://doi.org/10.1039/c0nr00541j>
- Pyshnaya IA, Razum KV, Poletaeva JE, Pyshnyi DV, Zenkova MA, Ryabchikova EI (2014) Comparison of behaviour in different liquids and in cells of gold nanorods and spherical nanoparticles modified by linear polyethyleneimine and bovine serum albumin. *Biomed Res Int* 2014:1–13. <https://doi.org/10.1155/2014/908175>
- Rasband WS (1997) ImageJ. In: U. S. National Institutes of Health, Bethesda, Maryland, USA. <http://imagej.nih.gov/ij/>
- Rojas-Andrade M, Cho AT, Hu P, Lee SJ, Deming CP, Sweeney SW, Saltikov C, Chen S (2015) Enhanced antimicrobial activity with faceted silver nanostructures. *J Mater Sci* 50(7):2849–2858
- Song WJ, Du JZ, Sun TM, Zhang PZ, Wang J (2010) Gold nanoparticles capped with polyethyleneimine for enhanced siRNA delivery. *Small* 6(2):239–246
- Sullivan MMO, Green JJ, Przybycien TM (2003) Development of a novel gene delivery scaffold utilizing colloidal gold-polyethyleneimine conjugates for DNA condensation. *Gene Ther* 10(22):1882–1890
- Sun XP, Dong SJ, Wang EK (2004) One-step synthesis and characterization of polyelectrolyte-protected gold nanoparticles through a thermal process. *Polymer* 45(7):2181–2184
- Sun XP, Dong SJ, Wang EK (2005) One-step preparation of highly concentrated well-stable gold colloids by direct mix of polyelectrolyte and HAuCl<sub>4</sub> aqueous solutions at room temperature. *J Colloid Interface Sci* 288(1):301–303
- Taylor U, Klein S, Petersen S, Kues W, Barcikowski S, Rath D (2010) Nonendosomal cellular uptake of ligand-free, positively charged gold nanoparticles. *Cytometry Part A* 77A (5): 439–446
- Thiramanas R, Laocharoensuk R (2016) Competitive binding of polyethyleneimine-coated gold nanoparticles to enzymes and bacteria: a key mechanism for low-level colorimetric detection of gram-positive and gram-negative bacteria. *Microchim Acta* 183(1):389–396. <https://doi.org/10.1007/s00604-015-1657-7>
- Thomas M, Klivanov AM (2003) Conjugation to gold nanoparticles enhances polyethyleneimine's transfer of plasmid DNA into mammalian cells. *Proc Natl Acad Sci U S A* 100(16): 9138–9143
- Wang ST, Yan JC, Chen L (2005) Formation of gold nanoparticles and self-assembly into dimer and trimer aggregates. *Mater Lett* 59(11):1383–1386

**Publisher's note** Springer Nature remains neutral with regard to jurisdictional claims in published maps and institutional affiliations.